Absence of correlation between built-in electric dipole moment and quantum Stark effect in InAs/GaAs self-assembled quantum dots

Weidong Sheng and Jean-Pierre Leburton
Beckman Institute for Advanced Science and Technology and Department of Electrical and Computer Engineering, University of Illinois at Urbana-Champaign, Urbana, Illinois 61801

We report significant deviations from the usual quadratic dependence of the ground state interband transition energy on applied electric fields in InAs/GaAs self-assembled quantum dots. In particular, we show that conventional second-order perturbation theory fails to correctly describe the Stark shift for electric field below $F = 10$ kV/cm in high dots. Eight-band $\mathbf{k}\cdot\mathbf{p}$ calculations demonstrate this effect is predominantly due to the three-dimensional strain field distribution which for various dot shapes and stoichiometric compositions drastically affects the hole ground state. Our conclusions are supported by two independent experiments.
PACS numbers: 78.67.Hc, 73.21.La, 31.15.Md

Self-assembled InAs/GaAs quantum dots (SADs) are three-dimensional (3D) semiconductor nanostructures in which electrons and holes are completely confined along the three dimensions of space by the band gap difference between InAs and GaAs materials [1]. In these nanoscale systems, the determination of the electronic spectra of both particles represents a major challenge because of the low symmetry of the 3D confined nanostructures that take (truncated) pyramidal or lens shapes, and are affected by the strong influence of strain due to the lattice mismatch between the InAs and GaAs crystals [2]. Experimentally, the difficulty of ascertaining the exact dot shape, and the non-uniformity in size distribution resulting from the growth process are also a handicap [3]. In this context, the knowledge of the respective positions of electrons and holes can provide information on the confining potential experienced by both particles, which is of primary importance for fundamental [4] as well as practical reasons [5].

It has been recently argued that because of the non-homogenous stoichiometric composition of SADs, resulting from atomic InAs-GaAs inter-diffusion, the center of mass of the ground state electrons and holes are displaced from one another with the hole above the electron, thereby inducing a built-in electric dipole oriented from the top to the base of the dot. This inverted electron-hole alignment [6] has been derived experimentally by assuming the usual linear relation between the electric dipole moment and the Stark shift in Stark effect spectroscopy on SADs in p-i-n structures, *i.e.*,

$$E(F) = E_0 + pF + \beta F^2 \qquad (1)$$

where E is the electron-hole ground state transition energy, p is the built-in dipole moment, and β measures the polarization of the electron and hole states.

By estimating the electric field at which the maximum transition energy occurs, one can determine whether the structure has a positive (if that happens at positive fields) or negative (if otherwise) built-in dipole moment. This quadratic dependence is well-known for quantum-well systems and has been confirmed in nanocrystallite quantum dots [7]. Recent theoretical works have made use of this linear relation to support the universality of the inverted alignment in SADs [8].

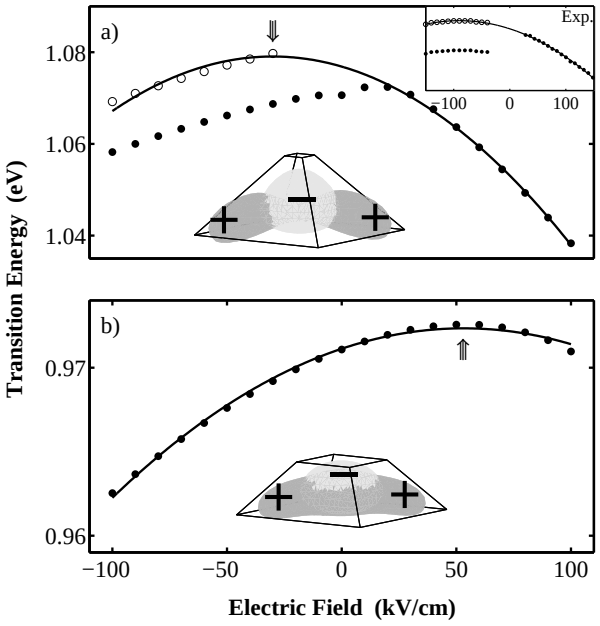

FIG. 1: Ground state interband transition energies as a function of electric fields for two truncated pyramidal self-assembled quantum dots. Probability density isosurfaces of the ground states of electron (dark grey) and hole (light grey) are shown on a schematic view of the structure. The calculated points are shown in dotted lines. a): The solid line is a fit to Eq. 1 using only the data at positive electric fields. The data at negative fields are shifted to the open dots by 11 meV to match the fitted curve. The top-right inset shows the corresponding experimental data taken from Ref. [6]. b): The solid line is a parabolic fit to all the data.

In this letter, we demonstrate that the linear relation between electric dipole moment and Stark shift as expressed in Eq. 1 is usually violated in SADs because of the unique strain field distribution in the dot, which strongly influences the rapidly varying confining potential for the holes. We show that this peculiar effect invalidates the conventional perturbation approach to establish the elec-

tric field dependence of the optical transition in SADs.

The system of SAD structures, containing both electrons and holes, can be well described by an eight-band strain-dependent $\mathbf{k}\cdot\mathbf{p}$ Hamiltonian [9], which reads,

$$(\mathbf{H}^0_{k\cdot p} + \mathbf{H}^s_{k\cdot p} + |e|Fz)\psi = E\psi. \quad (2)$$

Here $\mathbf{H}^0_{k\cdot p}$ and $\mathbf{H}^s_{k\cdot p}$ is the kinetic and strain-dependent part of the eight-band Hamiltonian [10], respectively, and $\psi = (\psi_1, \psi_2, \ldots, \psi_8)$ is the envelop eigenvector. By using continuum elasticity theory, the strain tensor is calculated on a large grid of $150\times150\times150$ sites. The Hamiltonian is then solved by Lanczos algorithm. The same technique has been successfully applied to study few-particle effect [11] and optical transitions [12] in quantum dots and very good agreement with experiments has been achieved.

Figure 1 shows the calculated dependence of interband transition energies on electric fields for two SAD structures. Fig. 1(a) illustrates the data for a $In_{0.8}Ga_{0.2}As$ dot with a constant composition throughout the structure. The pyramidal dot is 18 nm wide and 7.8 nm high, which is of similar size as that in the experiment of Fry *et al.* [6]. The electric field is applied vertically to the structure, pointing from the base to the top. For comparison, the corresponding experimental data is shown in the top-right inset.

An clear deviation from the quadratic dependence of the transition energy on the electric field is obtained from our numerical simulations that show two distinct branches, one for roughly each field direction, merging at around zero field. It is interesting to notice that, if the data at negative electric fields are shifted upwards by 11 meV, and if one ignores a few data points around zero-field, one can easily fit the remaining data with a single parabola characterized by a maximum at around $F = -40$ kV/cm. In this case, according to Eq. 1, the displaced curve yields a negative built-in dipole (-14 Å) in spite of the fact that the center of mass of the electron state is above that of the hole state by 7 Å as shown on the lower inset, thereby achieving normal alignment.

This fitting procedure was adopted by Fry *et al.* [6] to show the overall quadratic field dependence of the experimental transition energies (see upper right inset). The points marked with solid dots are the data measured from experiments. We notice however the structure may be of different stoichiometric composition than our SAD in Fig. 1(a). The authors shifted their data to the position marked with open dots to match the curve fitting from their data at positive electric fields. With this procedure, they claimed negative built-in dipole in the quantum dot structure. This experimental procedure was justified by the fact that for p-i-n structures, the Stark effect can only be measured under reverse biases. Therefore, given the asymmetric SAD shape and the fact that the Stark effect was measured for both field directions, two sets of samples i.e p-i-n and n-i-p structures, were used in the experiment.

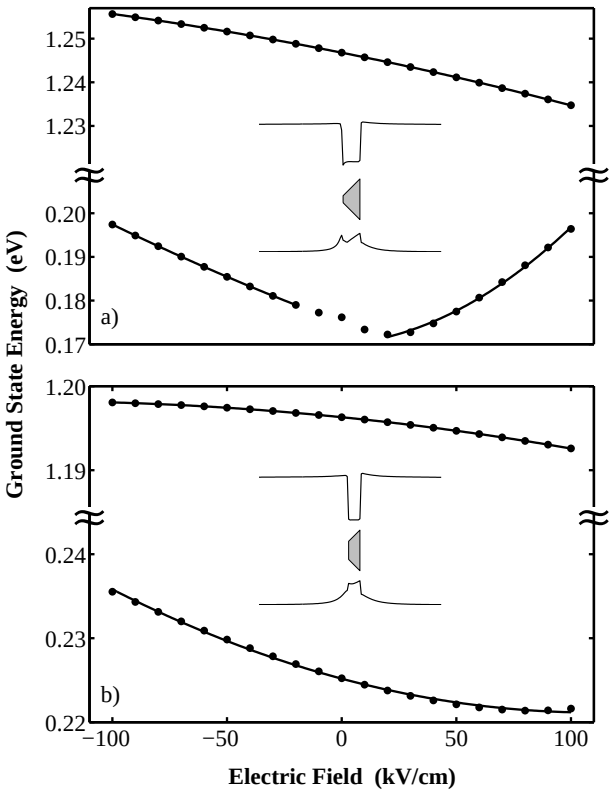

FIG. 2: Ground state energies of electrons and holes as a function of electric fields for the two quantum dots shown in Fig. 1. The band diagrams are shown in the insets.

While the conventional perturbation theory fails for the pyramidal quantum dot, it makes a successful prediction of Stark shifts for another quantum dot which is a largely truncated pyramidal InAs quantum dot shown in Fig. 1(b), which has the same base size, but is only 5.4 nm high. It has smaller transition energies than the pyramidal structure because of its uniform InAs composition. Unlike the dot shown in Fig. 1(a), it has nearly perfect quadratic dependence at electric fields as strong as $F = \pm100$kV/cm. The parameter extracted from the fitting curve gives a positive built-in dipole of 4.57 Å which agrees well with the actual value 4.8 Å.

In Fig. 2, we show the electron and hole ground state energies for the two structures as a function of electric fields. Electron energies for both structures are seen to have a linear profile with a slight bowing that can be well described by the usual quadratic dependence on the electric field, *i.e.*,

$$E_e(F) = E_e(0) + p_e F + \beta_e F^2, \quad (3)$$

in the second-order perturbation theory. The hole state in the truncated structure exhibits a similar feature and its energies can be well fitted with a parabola, *i.e.*,

$$E_h(F) = E_h(0) + p_h F + \beta_h F^2. \quad (4)$$

Here $p_{e(h)}/|e| = \langle\psi_{e(h)}|z|\psi_{e(h)}\rangle$ is the center of mass of

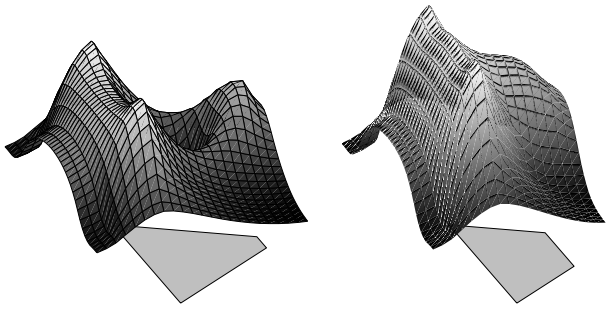

FIG. 3: Three-dimensional plots of strain distribution in a [100] plane across the center of quantum dots. Below the plots are the schematic view of cross sections of the structures.

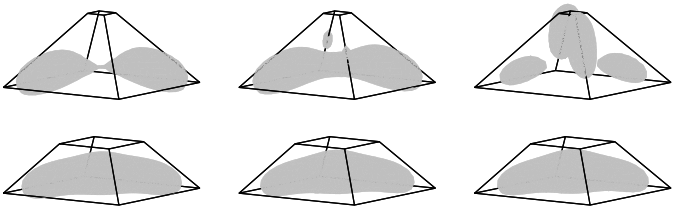

FIG. 4: Probability density isosurfaces of ground hole states at different electric fields, from left to right, −20 kV/cm, 10 kV/cm, and 20 kV/cm. Top panel: pyramidal dot (Fig. 1a); Bottom panel: truncated dot (Fig. 1b).

the electron (hole) state ψ_e (ψ_h) and $\beta_{e(h)}$ measures the polarization of the electron(hole) states. The correlation between the built-in dipole moment $p = p_e - p_h$ and quantum Stark effect is then obtained by taking the difference between the electron and hole energies to reflect Eq. 1. In the pyramidal dot, however, a quadratic fitting for the whole field range is not possible, although the left and right branches of the spectrum could be fitted piecewise by two parabolas, respectively.

The different behavior of electron and hole energies is attributed to their respective band edge profiles shown in the insets of Fig. 2. In both SADs, the conduction band edge is almost flat inside the dot with hard walls on the sides, which provides electrons a constant, strong confinement. Consequently, under the influence of external electric fields, electrons experience a smoothly varying confining potential inside the dot, which can be treated as a small perturbation with electron energies following the quadratic dependence given by Eq. 3. This type of behavior is also observed for holes in the truncated SAD structure (Eq. 4).

In the pyramidal dot, the valence band edge exhibits a more complicated, double-triangular profile with the lower part extending from the SAD base to about two-third of the structure hight, which effectively confines the ground hole state close to the bottom of the dot (see the inset in Fig. 1). Therefore, the holes are localized in a rapidly varying potential while the valence band edge changes abruptly close to the top of the structure. Hence, as vertical electric fields force the holes to move along the structure, they experience significantly different local confinement at different fields, which invalidates the perturbation approach as described in Eq. 1. This behavior is seen to occur at electric fields as low as $F = \pm 10$ kV/cm.

The rapidly varying confining potential which is responsible for the breakdown of the perturbation theory in the pyramidal structure is induced by the unique 3D strain field distribution within the SAD. Because the effect of other strain components on the valence bands are inferior in importance, we concentrate on the biaxial component of the strain which affects mostly the valence bands [13]. Fig. 3 shows a 3D plot of the magnitude of biaxial strain along a [100] plane across the center of the quantum dots. It is pointed out that the biaxial component of strain takes negative value inside the dot that is under biaxial compression and positive value in the barrier that is under biaxial tension.

Despite the fact that the structural difference between the two dots results only from the truncation, both structures exhibit substantially different strain distribution. The biaxial strain distribution in the pyramidal dot shows rapid variation inside the structure along the growth direction while the truncated dot exhibits a smoother profile. The strain field is so coherent that the tip of the pyramidal dot has a significant effect on the whole strain distribution.

In Fig. 4, we show the ground hole states at both negative and positive electric fields for the two structures. For the pyramidal structure of Fig. 1(a), the wave function at negative field $F = -20$ kV/cm looks similar to that at zeros field except that it is localized closer to the dot bottom. At a positive field $F = 10$ kV/cm, the hole wave function develops a pair of small 'wings' around the facet edges [14]. Because of a strong local confinement imposed by the sharp triangular potential (see the band diagram inset in Fig. 2), the hole state could not extend into the upper half part of the structure as electron states do. At a stronger positive field $F = 20$ kV/cm, these wings even dominate over the other portions of the wave function.

The obvious asymmetric behavior of the ground hole states implies that the corresponding wave functions cannot be expanded to the first order in the electric field as

$$\psi_h(F) = \psi_h(0) + \phi_h F, \tag{5}$$

which would result into symmetric wave functions with respect to positive and negative electric fields for the whole range of electric fields. Instead, if we chose different values of the perturbation, ϕ_h, for negative and positive fields, respectively, it is possible to fit the hole energies with two parabolas (see Fig. 2).

In the truncated structure, the hole states are seen to have a different probability density distribution. The wave functions change very smoothly with the electric fields, because of a relatively flat valence band edge (see Fig. 2 inset). In addition, the lateral confinement close to the SAD top is also weaker compared with that in the

TABLE I: Calculated built-in dipole moments and their fitted values from the assumed quadratic dependence on the field for various quantum dot structures. All the lengths are expressed in nm. If not specified, all structures are homogeneous InAs/GaAs dots.

Size	Actual value	Fitted value
18×7.8^a	-0.31	N/A
18×7.8^b	0.70	-1.40
18×7.8	0.33	-1.23
18×9.0	0.36	-1.33
18×6.6	0.54	0.39
18×5.4	0.46	0.48

[a]Inhomogeneous InAs dot with two interdiffused monolayers, $In_{0.6}Ga_{0.4}As$ and $In_{0.8}Ga_{0.2}As$, in the bottom.
[b]The $In_{0.8}Ga_{0.2}As$ dot shown in Fig. 1(a).

pyramidal SAD as shown Fig. 1. Therefore, hole states behave coherently throughout the whole range of electric fields, exhibiting nearly perfect quadratic dependence of their eigen energies on electric fields.

Table I lists the actual and fitted values of dipole moment for several SADs. All structures have the same base dimensions, but different heights or composition profiles. It should be stressed that the fitted values are obtained from the model data only for positive electric fields, *i.e.*, the right branch of the spectrum. Except for the last structure, all values exhibit large discrepancy between the fitted curve and the model (calculated) data at negative fields. The first structure has a negative built-in dipole induced by the inhomogeneous diffusion [15], responsible for two bumps in the transition energy for positive and negative fields, which makes the fitting over a broad field range, meaningless. This structure is similar to the SADs investigated recently by Chen *et al.* [16] where a negative dipole moment was extracted (the orientation of their field was opposite to ours) from a quadratic fitting over a smaller range of field (-7.5 kV/cm $\leq F \leq$ 10 kV/cm), in good agreement with our data. The next three structures have homogeneous composition, and all exhibit positive dipoles. However, the fitted values for these structures are all negative. Therefore, it is a general feature of high pyramidal quantum dots with less than 25% truncation to exhibit erroneously a 'negative' built-in dipole when fitted to the Stark shifts. The fourth structure has about 27% truncation with a dipole larger than those in the two previous dots. The corresponding fitted value is positive but is 30% smalled than the actual value. In the last structure, which is strongly truncated, the difference between the actual value and the fitted one becomes negligible.

In conclusion, we have shown that the unique 3D strain field distribution is responsible for the breakdown of the linear dependence of the built-in electric dipole moment in the Stark shift in SADs. This effect is mostly noticeable in high SADs where holes are mostly affected by rapidly varying components of the strain induced confining potential, which invalidates the second order perturbation theory. While perturbation theory is expected to fail at strong electric fields, we point out that significant deviations from the usual Stark effect already occur at fields lower than $F = 10$ kV/cm. For largely truncated or flat SADs, the Stark shift retains its usual quadratic dependence on external fields.

Acknowledgments

This work is supported by Army Research Office, grant #DAAD 10-99-10129 and National Computational Science Alliance, grant #ECS000002N.

[1] D. Bimberg, M. Grundmann, and N. N. Ledentsov, *Quantum Dot Heterostructures* (John Wiley & Sons, UK, 1998).
[2] I. Kegel, *et al.*, Phys. Rev. Lett. **85**, 1694 (2000).
[3] Y. Ebiko, *et al.*, Phys. Rev. Lett. **80**, 2650 (1998).
[4] D. Gammon, *Nature* **405**, 899 (2000).
[5] D. G. Deppe and D. L. Huffaker, Appl. Phys. Lett. **77**, 3325 (2000).
[6] P. W. Fry, *et al.*, Phys. Rev. Lett. **84**, 733 (2000).
[7] S. A. Empedocles and M. G. Bawendi, *Science* **278**, 2114 (1997).
[8] J.A. Barker and E.P. O'Reilly, Phys. Rev. B **61**, 13840 (2000).
[9] T. B. Bahder, Phys. Rev. B **41**, 11992 (1990).
[10] C. Pryor, Phys. Rev. Lett. **80**, 3579 (1998).
[11] L. Landin, M. S. Miller, M.-E. Pistol, C. E. Pryor, and L. Samuelson, *Science* **280**, 262 (1998).
[12] W. Sheng and J.-P. Leburton, Appl. Phys. Lett. **80**, 2755 (2002).
[13] T. B. Bahder, Phys. Rev. B **45**, 1629 (1990).
[14] C. Pryor, M.-E. Pistol, and L. Samuelson, Phys. Rev. B **56**, 10404 (1997).
[15] W. Sheng and J.-P. Leburton, Phys. Rev. B, **63**, 161301R (2001).
[16] Z. Chen, E.-T. Kim, and A. Madhukar, Appl. Phys. Lett. **80**, 2770 (2002).